CHEMISTRY
A EUROPEAN JOURNAL

DOI: 10.1002/chem.200902559

Control of Biocatalytic Transformations by Programmed DNA Assemblies

Ronit Freeman, Etery Sharon, Carsten Teller, and Itamar Willner*[a]

Abstract: This study demonstrates the self-assembly of inhibitor/enzyme-tethered nucleic acid fragments or enzyme I-, enzyme II-modified nucleic acids into functional nanostructures that lead to the controlled inhibition of the enzyme or the activation of an enzyme cascade. In one system, the anti-cocaine aptamer subunits are modified with monocarboxy methylene blue (MB^+) as the inhibitor and with choline oxidase (ChOx). The cocaine-induced self-assembly of the aptamer subunits complex results in the inhibition of ChOx by MB^+. In a further configuration, two nucleic acids of limited complementarity are functionalized at their 3′ and 5′ ends with glucose oxidase (GOx) and horseradish peroxidase (HRP), respectively, or with MB^+ and ChOx. In the presence of a target DNA sequence, synergistic complementary base-pairing occurs, thus leading to stable supramolecular Y-shaped nanostructures of the nucleic acid units. A GOx/HRP bienzyme cascade or the programmed inhibition of ChOx by MB^+ is demonstrated in the resulting nucleic acid nanostructures. A quantitative theoretical model that describes the nucleic acid assemblies and that results in the inhibition of ChOx by MB^+ or in the activation of the GOx/HRP cascade, respectively, is provided.

Keywords: aptamers · cocaine · DNA · enzymes · inhibitors

Introduction

The self-organization of nucleic acids into functional supramolecular structures has attracted substantial research efforts over the last decade.[1] As one prime example, the self-assembly of nucleic acid fragments into catalytic DNAzyme units was used to create inducible catalytic labels and to develop various amplified sensors.[2] The formation of supramolecular complexes between aptamer subunits and their substrates has enabled the design of optical and electrochemical sensors.[3] Similarly, the organization of supramolecular DNA structures allowed the design and activation of different DNA machines, such as "walkers"[4] or "tweezers".[5] The programmed mechanical interconversion of the DNA nanostructures has been used to perform logic-gate operations[6] and has been suggested as a future means for nanomedicine.[7] Furthermore, DNA scaffolds have been used to assemble enzymes through directed hybridization, and the systems have been used to activate enzyme cascades.[8] Recently, it has been reported that the self-assembly of enzyme-modified anti-cocaine aptamer subunits—modified at their 3′ and 5′ ends with enzymes—into a supramolecular aptamer/cocaine complex resulted in a communication between the tethered enzymes and the activation of a biocatalytic cascade.[9] Also, the self-organization of Y-shaped armed nucleic acid structures provided a configuration for the fluorimetric detection of DNA.[10]

Herein, we present programmed assemblies of supramolecular complexes of nucleic acids that do not only allow the activation of enzyme cascades, but permit the controlled inhibition of enzymes—processes that do not occur (under similar experimental conditions) in a diffusion-controlled homogeneous mixture of the biomolecular components. We demonstrate that aptamer subunits or two nucleic acid subunits tethered to an enzyme and an inhibitor self-assemble into aptamer/ligand complexes or are bridged by a complementary nucleic acid into Y-shaped structures, in which the enzyme is inhibited. Furthermore, we show that the tethering of two enzymes to the nucleic acid units that are bridged into the Y-shaped nanostructure by the complementary oligonucleotide allows the activation of a biocatalytic cascade of the two enzymes. In addition, we formulate a quantitative model that describes the inhibition phenomena or the enzyme cascades in the different supramolecular structures of the nucleic acids.

[a] R. Freeman, E. Sharon, Dr. C. Teller, Prof. I. Willner
Institute of Chemistry
The Hebrew University of Jerusalem
Jerusalem 91904 (Israel)
Fax: (+972) 2-652-7715
E-mail: willnea@vms.huji.ac.il

Supporting information for this article is available on the WWW under http://dx.doi.org/10.1002/chem.200902559.

WILEY InterScience DISCOVER SOMETHING GREAT
© 2010 Wiley-VCH Verlag GmbH & Co. KGaA, Weinheim

Results and Discussion

Enzyme/inhibitor-modified aptamer subunits: The anti-cocaine aptamer subunits were functionalized at their 3′ and 5′ ends with monocarboxy methylene blue (MB^+) and choline oxidase (ChOx) to yield MB^+- and ChOx-modified strands **1** and **2**, respectively. Spectroscopic analysis indicated that the average loading of ChOx corresponded to one nucleic acid residue per protein. The nucleic acid-functionalized ChOx exhibited approximately 92% of the native enzyme activity (synthesis of the modified ChOx, determination of the loading, and enzyme-activity assays are provided in the Experimental Section and Supporting Information). MB^+ is known to inhibit ChOx.[11] Indeed, the addition of cocaine to a system that consists of the MB^+-functionalized aptamer subunit **1** and the ChOx-modified aptamer subunit **2** assembles the supramolecular aptamer/cocaine complex and results in the inhibition of ChOx (Scheme 1).

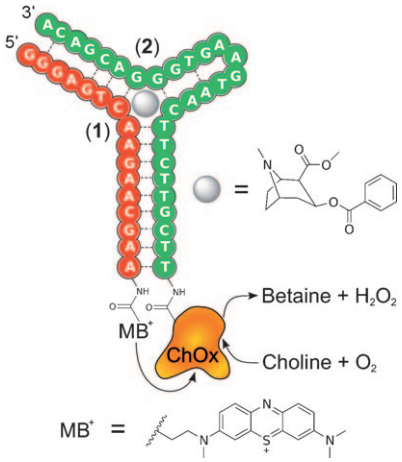

Scheme 1. Cocaine-induced self-assembly of enzyme/inhibitor-tethered aptamer fragments that yields the controlled inhibition of biocatalytic activity. Strand **1** was linked to MB^+ and oligonucleotide **2** was coupled by a bis(sulfosuccinimidyl) suberate BS^3 linker to ChOx.

The activity of ChOx was monitored by assaying the hydrogen peroxide generated by the ChOx-mediated oxidation of choline to betaine with oxygen by using a secondary colorimetric assay that applied the horseradish peroxidase (HRP)-catalyzed oxidation of 2,2′-azino[bis(3-ethylbenzthiazoline-6-sulfonic acid)] ($ABTS^{2-}$) by H_2O_2 to form the colored $ABTS^{\bullet-}$ species, which was monitored at $\lambda = 414$ nm.

Figure 1 depicts the rates of the oxidation of choline in the presence of different concentrations of cocaine. Curve a in Figure 1 shows the time-dependent absorbance change generated by ChOx-modified strand **2** in the absence of MB^+-modified strand **1**. This maximum enzymatic activity was recorded in the presence of 25 mM choline with no added cocaine. Upon the addition of MB^+-linked oligonucleotide **1**, a small depletion of the absorbance is observed (Figure 1, curve b), thus implying that the inhibition of ChOx by MB^+ is not efficient under these experimental conditions. Curves c–j in Figure 1 show the time-dependent

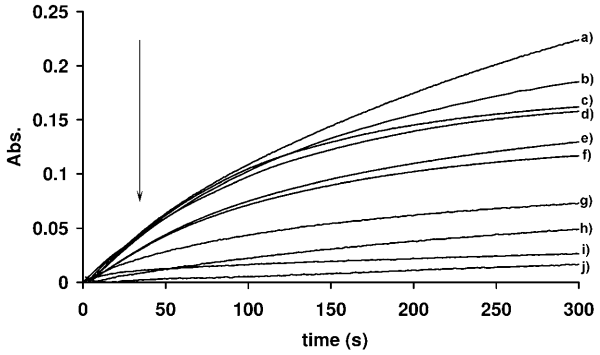

Figure 1. Time-dependent absorbance changes that correspond to the oxidation of the $ABTS^{2-}$ species by the ChOx/MB^+ system activated by the supramolecular aptamer complex generated in the presence of various concentrations of cocaine. a) Only ChOx-modified oligmer **2**, b) 0, c) 1×10^{-8}, d) 5×10^{-8}, e) 1×10^{-7}, f) 5×10^{-7}, g) 1×10^{-6}, h) 1×10^{-5}, i) 1×10^{-4}, j) 1×10^{-3} M. The respective concentrations of the aptamer subunits **1** and **2** were 5×10^{-8} M. All the experiments were performed in phosphate buffer (10 mM, pH 7.4, 100 mM NaCl).

spectral changes of the system upon the addition of different concentrations of cocaine to the mixture of MB^+-modified strand **1** and ChOx-modified strand **2**. As the concentration of cocaine increases, the degree of inhibition rises. This outcome is consistent with the fact that as the concentration of cocaine is elevated, the content of the supramolecular aptamer/cocaine complex increases, thus resulting in a high local concentration of MB^+ within the proximity of the enzyme. This behavior leads to the efficient inhibition of ChOx. Control experiments revealed that cocaine by itself has no effect on the activity of ChOx and that cocaine in the presence of a foreign, MB^+-modified DNA has no influence on the ChOx-modified strand **2**. The analysis of the activity of ChOx in the presence of different concentrations of cocaine indicates an apparent dissociation constant of cocaine that corresponds to $K_D = 0.66$ μM. This value is substantially lower than the dissociation constant of the cocaine/aptamer complex ($K_D \approx 200$ μM)[12] or the inhibition constant of MB^+ for ChOx in solution ($K_i = 74$ μM).[11] This difference is caused by the binding mechanism, which does not resemble a standard one-to-one interaction, but instead is explained much better by a cooperative binding mechanism (see the section on the quantitative evaluation of the DNA complexes).

We examined the specificity of the system to cocaine. It has been reported that the methylecgonine, generated by the enzymatic hydrolysis of the benzoyl ester moiety of cocaine, has a lower affinity to the aptamer fragments.[12] Accordingly, treatment of the inhibited ChOx system in the supramolecular structure of the cocaine/aptamer subunits with butyrylcholinesterase results in the partial separation of the aptamer/cocaine complex and the reactivation of the ChOx activity (Figure 2). In phase I, that is, in the presence of 1×10^{-3} M cocaine, an effective 80% inhibition of ChOx by MB^+ takes place due to the formation of the cocaine/aptamer complex. The butyrylcholinesterase is added in phase II. This results in the reactivation of the ChOx cata-

 © 2010 Wiley-VCH Verlag GmbH & Co. KGaA, Weinheim

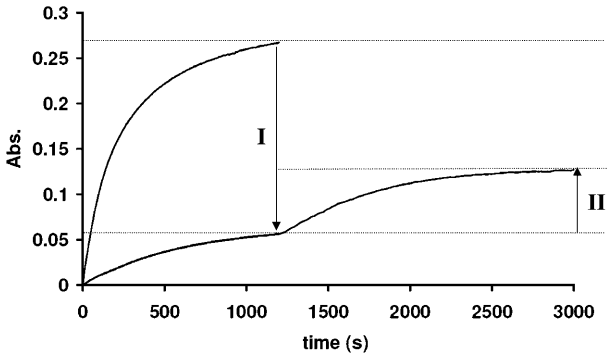

Figure 2. Inhibition and reactivation of ChOx activity. Phase I: inhibition of the activity of ChOx-modified strand **2** by MB^+-modified strand **1** during the supramolecular assembly of the aptamer subunits and in the presence of cocaine (1×10^{-3} M). Phase II: partial restoration of ChOx activity after the addition of the hydrolytic enzyme butyrylcholinesterase.

lytic activity. The incomplete recovery (approximately 50%) of the activity of ChOx might be attributed to the low hydrolysis rate of cocaine by butyrylcholinesterase[13] and/or to a low affinity of the hydrolytic product to the aptamer subunits,[12] which generates a low concentration of the supramolecular complex that still inhibits ChOx.

Furthermore, we confirmed that the spatial organization of the enzyme and inhibitor in close proximity is essential to activate the enzyme inhibition. Toward this goal, we used ChOx-tethered nucleic acid **1** as one component and covalently attached MB^+ to nucleic acid **3**. The latter nucleic acid is fully complementary to **1**, in which the characteristic aptamer loop is eliminated. The spatial organization of ChOx/MB^+ by the DNA duplex structure **1**/**3**, indeed, causes the inhibition of the biocatalytic process with an efficiency comparable to high concentrations of cocaine (see Figure 1S in the Supporting Information).

It should be noted that the inhibition of the biocatalytic transformation by the cocaine-induced assembly of the supramolecular complex might also be viewed as a method for the amplified detection of cocaine. In fact, this method enabled the analysis of cocaine with a detection limit corresponding to 1×10^{-8} M.

Enzyme-cascade-modified Y-shaped DNA structure: The second configuration (Scheme 2) comprises two nucleic acids of limited complementarity that are designed to capture a specific target DNA sequence. The base-pairing complementarity of **4** and **5** is insufficient to maintain a stable duplex structure of the two nucleic acids at room temperature. The two probe strands **4** and **5** were modified at their 3′ or 5′ ends with glucose oxidase (GOx) or HRP, respectively (see the Experimental Section for the synthesis of the functionalized nucleic acids). In the presence of the target nucleic acid **6**, the GOx-modified strand **4** and HRP-linked strand **5** arrange the two enzymes in close proximity (Scheme 2A).

Figure 3 shows the activation of the biocatalytic cascade of the two enzymes upon the bridging of the **4**/GOx and **5**/HRP components by the target **6**. The activity of the cascade was monitored by the peroxidase-catalyzed oxidation of the $ABTS^{2-}$ ion to the colored $ABTS^{\bullet-}$ species. The secondary HRP substrate, hydrogen peroxide, was provided by GOx. This enzyme uses molecular oxygen to oxidize glucose and yields gluconic acid and the necessary H_2O_2. Only the

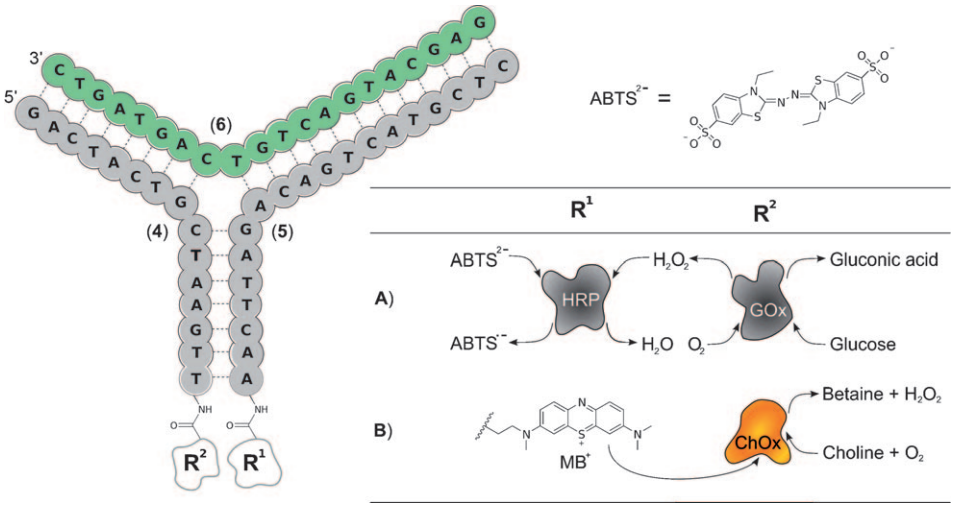

Scheme 2. The self-assembly of enzyme/enzyme or enzyme/inhibitor-tethered DNA fragments into Y-shaped DNA. A) Enzyme cascade of GOx and HRP and B) inhibition of ChOx by MB^+.

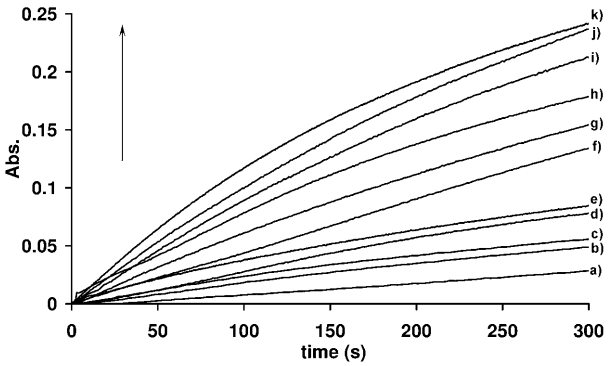

Figure 3. Time-dependent absorbance changes that correspond to the oxidation of the $ABTS^{2-}$ species by the GOx/HRP enzyme cascade activated by the Y-shaped DNA duplex generated by variable concentrations of **6**. a) No target **6**, b) 1×10^{-11}, c) 5×10^{-11}, d) 1×10^{-10}, e) 5×10^{-9}, f) 1×10^{-9}, g) 5×10^{-9}, h) 1×10^{-8}, i) 5×10^{-8}, j) 1×10^{-7}, k) 5×10^{-7} M. All the experiments were performed with a respective probe strand concentration of 5×10^{-8} M and in phosphate buffer (10 mM, pH 7.4, 100 mM NaCl).

 © 2010 Wiley-VCH Verlag GmbH & Co. KGaA, Weinheim

close proximity of both enzymes and a high local concentration of H_2O_2 allow the activation of the bienzyme cascade. In the absence of **6**, only a very low turnover is recorded (Figure 3, curve a). This outcome confirms that the two enzymes hardly communicate with each other without the formation of a stable nucleic acid assembly. The bienzyme cascade is only activated in the presence of target oligonucleotide **6**. As the concentration of **6** increases, the bienzyme cascade turnover is enhanced (Figure 3, curves b–k). Control experiments reveal that a foreign nucleic acid that lacks complementarity to **4** and **5** does not activate the bienzyme cascade. These results indicate that the hybridization of **6** with **4**/GOx and **5**/HRP leads to the supramolecular nucleic acid assembly that brings the two enzymes into proximity, thus allowing the activation of the bienzyme cascade.

Further support for the significance of the Y-shaped-induced proximity effect on the activation of the enzyme cascade consisting of GOx/HRP was obtained by studying the effect of added catalase on the turnover of the enzyme cascade activated on the Y-shaped DNA structure, and on the enzyme cascade in solution. Catalase disproportionates H_2O_2, hence, it is anticipated to scavenge the GOx-generated H_2O_2, thus decreasing the yield of the $ABTS^{\bullet-}$ species. Figure 4A shows the time-dependent absorbance changes generated by the free enzymes GOx and HRP (each at a concentration of 1×10^{-8} M) in the absence and presence of catalase (2×10^{-8} M; Figure 4A, curves a and b, respectively). The absorbance of the $ABTS^{\bullet-}$ species formed after approximately 400 seconds is significantly lower in the presence of catalase corresponding to approximately 50% inhibition of the cascade upon the addition of catalase (Figure 4B). Figure 4A shows the time-dependent formation of the $ABTS^{\bullet-}$ species in the presence of the Y-shaped DNA structure (each nucleic acid-modified enzyme at a concentration of 1×10^{-8} M) in the absence of catalase (Figure 4A, curve c) and in the presence of added catalase (concentration: 1×10^{-8} and 2×10^{-8} M; Figure 4A, curves d and e, respectively). We realize that in the presence of the Y-shaped DNA structure the enzyme cascade is inhibited only by 20% in the presence of 2×10^{-8} M catalase (relative to 50% inhibition of the cascade in solution; Figure 4B). These results are consistent with the expected influence of the proximity effect on the activation of the enzyme cascade. Whereas in solution, catalase scavenges the diffusive H_2O_2 effectively, thus leading to the effective inhibition of the biocatalytic cascade. However, the diffusional catalase cannot efficiently scavenge the H_2O_2 generated by GOx in the Y-shaped structure relative to the effective uptake of H_2O_2 by the adjacent HRP. As a result, the GOx/HRP cascade is less affected by added catalase.

Although our discussion emphasized the use of the three-arm DNA structure for the activation of the enzyme cascade, one may consider this system also as a sensor configuration for the amplified detection of nucleic acid **6** by the enzyme cascade. The detection limit for the sensing of target nucleic acid **6** by the enzyme cascade is 1×10^{-11} M. Another advantage of the configuration presented herein

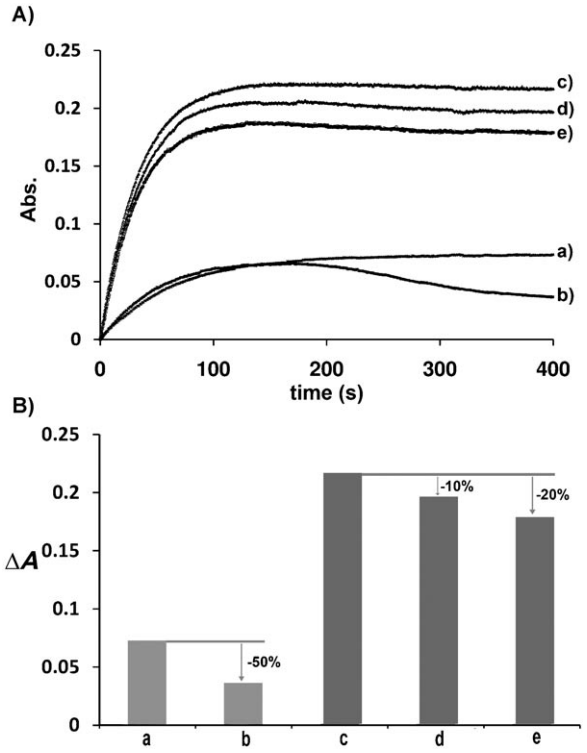

Figure 4. A) Time-dependent absorbance changes that correspond to the oxidation of the $ABTS^{2-}$ species by a) the free enzymes GOx/HRP in the absence of catalase; b) the free enzymes GOx/HRP in the presence of catalase (2×10^{-8} M); c) the GOx/HRP enzyme cascade activated by the Y-shaped DNA structure in the absence of catalase; d) the GOx/HRP enzyme cascade activated by the Y-shaped DNA structure in the presence of catalase (1×10^{-8} M); e) the GOx/HRP enzyme cascade activated by the Y-shaped DNA structure in the presence of catalase (2×10^{-8} M). All the experiments were performed with a respective probe strand concentration of 1×10^{-8} M in phosphate buffer (10 mM, pH 7.4, 100 mM NaCl). B) Comparison between the different final absorbance changes (ΔAbs at 400 s) of the respective systems shown in A.

rests on the fact that only a very low background signal is observed in the absence of the analyte **6**.

It should be noted that the Y-shaped DNA structure is asymmetric and the left arm of the supramolecular structure includes only eight base pairs, whereas the right arm of the structure includes twelve base pairs. This model was purposely designed to achieve the desired DNA supramolecular nanostructures. The eight-base complementarity is insufficient to stabilize the left-arm duplex structure at room temperature. On the other hand, the twelve-base complementarity between **5** and **6** can stabilize the duplex structure to form the right arm of the assembly. The secondary association of **4** to the preformed duplex **5**/**6** is stabilized by the synergetic base pairing of the complementary domains of **4** with **5** and **6**, respectively. This programmed assembly of the structure prevents the formation of aggregated, multimeric nanostructures through intermolecular hybridizations of the three components. Indeed, gel-electrophoretic studies reveal the formation of pure Y-shaped DNA structures without any aggregated by-products (see Figure 2S in the Supporting Information).

 © 2010 Wiley-VCH Verlag GmbH & Co. KGaA, Weinheim

Enzyme/inhibitor-modified Y-shaped DNA structure: Following the paradigm of the assembly of aptamer subunits studied previously,[8] and herein, we also modified the two probe strands **4** and **5** with an enzyme and its inhibitor (i.e., ChOx and MB^+, respectively). The interaction with the target nucleic acid **6** leads to the assembly of the supramolecular Y-shaped structure and, consequently, to the inhibition of ChOx activity by MB^+ (Scheme 2B). The biocatalytic turnover of ChOx was monitored by the oxidation of choline to betaine and the concurrent reduction of oxygen to hydrogen peroxide. The formation of H_2O_2 allowed the peroxidase-catalyzed oxidation of $ABTS^{2-}$ ions to the colored $ABTS^{\bullet-}$ species, which was measured spectrophotometrically at $\lambda = 414$ nm.

Figure 5 depicts the rate of the oxidation of choline in the presence of different concentrations of **6**. The inhibition of ChOx was induced by assembly of the three-arm duplex

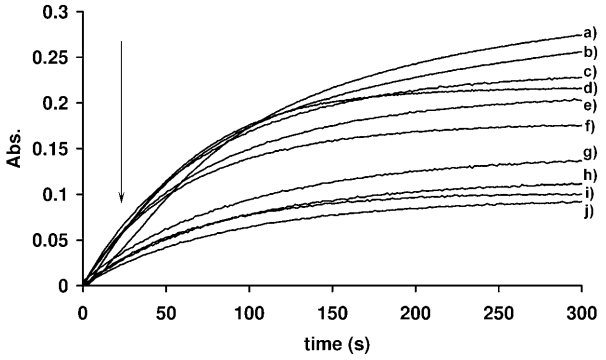

Figure 5. Time-dependent absorbance changes that correspond to the oxidation of the $ABTS^{2-}$ species by the ChOx/MB^+ system activated by the Y-shaped DNA structure generated by variable concentrations of nucleic acid **6**. a) Only ChOx-modified strand **4**, b) 0, c) 1×10^{-10}, d) 5×10^{-10}, e) 1×10^{-9}, f) 5×10^{-9}, g) 1×10^{-8}, h) 5×10^{-8}, i) 1×10^{-7}, j) 5×10^{-7} M. All the experiments were performed with a respective probe strand concentration of 5×10^{-8} M and in phosphate buffer (10 mM, pH 7.4, 100 mM NaCl).

structure consisting of ChOx-functionalized strand **4** and MB^+-functionalized strand **5** bridged by the target nucleic acid **6**. The maximum activity of ChOx is achieved when only the ChOx-functionalized nucleic acid **4** is present in the sample (Figure 5, curve a). The activity decreases slightly upon addition of the second MB^+-labeled oligonucleotide **5** (Figure 5, curve b). This outcome can be explained by the existence of a small fraction of a dimeric complex of **4** and **5** despite the limited complementarity and the low concentration of the two nucleic acids. As the concentration of **6** increases, the degree of inhibition of ChOx increases further (Figure 5, curves c–j), thus implying that the close proximity of the MB^+ inhibitor to ChOx controls the efficiency of the inhibition process.

Quantitative evaluation of the binding features of the aptamer subunits and the Y-shaped DNA complexes: As stated earlier, the detection limit for cocaine using the assembly of the aptamer subunits upon ligand binding is substantially lower than what could be expected from the affinity binding constant of the aptamer toward cocaine. In fact, a simple logistic fit (similar to antigen/antibody binding phenomena) of the experimental absorbance data reveals an apparent dissociation constant K_D of 0.66 μmol L^{-1} (see Table 1 and the Supporting Information). This value is approximately 400-fold lower relative to the reported value of 200 μM.[12] We also observed a Hill slope that is not unity ($p = 0.59$). These facts indicate that the examined binding and assembly does not follow a simple one-to-one binding model. We attempted to develop a quantitative model that may explain the experimental results to account for this apparent discrepancy. The aptamer/ligand complex and the Y-shaped bridged nucleic acid structure share a common binding feature that is represented by the assembly of the three components. The quantitative model should, therefore, take into account the different possible interactions among all the components. Furthermore, one should realize that in the inhibition systems, the inhibitor could provide an additional driving force to the formation of the resulting supramolecular structures. We adapted the method described for the association of G-protein-coupled receptor (GPCR) complexes to formulate the binding model in our systems. The allosteric behavior of GPCR is characterized by the binding of an orthosteric ligand **A** to the receptor **R** in the presence or absence of an allosteric modulator **B**.[14] Usually, **A** is a low-molecular-weight compound (e.g., serotonin) that binds to a specific receptor **R**. The affinity toward the receptor can be altered through the binding of a secondary ligand. This ligand **B** can be a low-molecular-weight substance, another protein, or biopolymer (e.g., oleamide, G-protein, or heparin, respectively).[15]

Table 1. Obtained parameters after nonlinear curve fitting of the cocaine binding by the ChOx/MB^+-modified aptamer subunits.[a]

	Logistic fit	Ternary complex
K_H [μmol L^{-1}]	–	0.19
K_T [μmol L^{-1}]	–	4.5
α'	–	25.1
$E_{max,1}$	0.177[b]	0.203
$A2$	0.017	–
x_0 [μmol L^{-1}]	0.66	–
p	0.59	–
reduced χ^2	1.477×10^{-4}	1.899×10^{-4}

[a] Comparison of the standard logistic fit versus the binding model for the ternary complex assembly by using Equation (1). [b] This value is the upper limit (A1) of the logistic fit for comparison.

This model was adapted to evaluate the binding features of the cocaine/aptamer complex. In particular, the ChOx-labeled subunit **2** (H_I) resembles the receptor because it provides the measured signal and both of the other two components bind to it. The second aptamer subunit **1** (H_{II}) was modified with MB^+ and works as the orthosteric ligand, as the binding of MB^+ to the enzyme directly alters the activity of the enzyme. Thus, the fraction of MB^+-labeled H_{II} bound to H_I represents the receptor occupancy by its ligand.

 © 2010 Wiley-VCH Verlag GmbH & Co. KGaA, Weinheim

The target molecule cocaine (T) acts as the allosteric modulator by mediating the assembly of the ternary complex. Similarly, the target DNA sequence can aid the formation of the Y-shaped DNA complex based on the two probe strands. In this case, the target nucleic acid acts as the allosteric ligand and modulates the channeling of H_2O_2 from the GOx-modified strand **4** to the HRP-labeled strand **5**. Scheme 3 shows the possible reaction pathways for the formation of the ternary complex assembly. For clarity, both aptamer subunits or probe strands are treated as identical with regard to their individual binding affinities. (It should be noted that the three-component complexes discussed in the present study can, in principle, be formed by three alternative stepwise paths. However, it is insignificant by which pathway the final complex is formed. Furthermore, the cooperativity factors of all three paths are identical. See the Supporting Information for the mathematical elucidation of these features.)

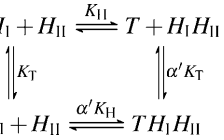

Scheme 3. Reaction pathway for the ternary complex assembly of the two subunits (H_I and H_{II}: aptamer subunits or DNA probe strands) and their target (T: cocaine or DNA).

Two affinity constants are necessary to describe the system: K_H is the dissociation constant for the oligonucleotide subunits and K_T is the dissociation constant of the target from the subunit strand. Furthermore, α' is introduced and represents the so-called cooperativity factor. In analogy to the equations used to fit the fractional receptor occupancy depending on the agonist concentration,[13] we derived the concentrations of the assembled supramolecular complexes of the enzymatic systems, where $i(x)$ [Eq. (1)] corresponds to the concentration of the assembled inhibition-based supramolecular structure, that is, ChOx/MB$^+$, and $c(x)$ [Eq. (2)] corresponds to the concentration of the assembled nanostructure that activates the bienzyme cascade GOx/HRP [see the Supporting information for a detailed derivation of the relationships given by Equations (1)–(3)].

$$y = i(x) = E_{max1}\left(1 - \frac{H}{H + K_{app}}\right) \quad (1)$$

$$y = c(x) = \frac{E_{max2} \cdot H}{H + K_{app}} \quad (2)$$

$$K_{app} = K_H \cdot \frac{1 + x/K_T}{1 + \alpha' \cdot x/K_T} \quad (3)$$

Here H represents the concentration of the ChOx- or HRP-modified DNA strands. This value is a constant, which is set by the experimental conditions to 50 nM. The E_{max} values constitute the maximum enzymatic turnover. In the case of the inhibition with MB$^+$, this value represents the activity of the ChOx-modified strand in the absence of the MB$^+$-linked oligonucleotide. In case of the enzyme cascade, the maximum value is reached at complete saturation of the probe strands with the target DNA. The independent variable x describes the concentration of the target, namely, cocaine or the bridging DNA **6**.

Equation (3) shows that the observed, apparent dissociation constant K_{app} is a composite parameter that depends on the concentration of the target, the binding constant K_T, and the cooperativity factor α'. If there is a positive cooperative interaction ($\alpha' > 1$), the observed binding will be stronger (i.e., $K_{app} < K_H$). As a result, the dose–response curve will be shifted to lower concentrations (see the Supporting Information for simulated curves). The opposite effect occurs in the case of negative cooperativity ($\alpha' < 1$). An apparently weaker binding ($K_{app} > K_H$) results in a right-shift of the curve to higher concentrations (see the Supporting Information).

The model for the ternary complex assembly also provides reasonable explanations for the upper and lower limits of the sigmoidally shaped curve. The upper and lower limits (A1 and A2, respectively) of the standard logistic fit are usually interpreted as saturation of the system and background signal, respectively. In the case of the ternary complexes, these limits largely depend on the K_H value, the affinity between the two aptamer subunits or both probe strands, and the cooperativity factor α'. As the target concentration decreases, the apparent dissociation constant K_{app} approaches the value of K_H. For infinitely high concentrations of T, on the other hand, K_{app} equals the ratio of K_H and the cooperativity factor [Eq. (4)].

$$\lim_{T \to 0} K_{app} = K_H \text{ and } \lim_{T \to \infty} K_{app} = K_H/\alpha' \quad (4)$$

This behavior explains the observed drop in activity of the ChOx-modified oligomer (which represents $E_{max,1}$) when the MB$^+$-linked nucleic acid is added. Even at a target concentration of zero, a fraction of the aptamer subunits or probe strands will assemble as a binary complex, thus decreasing the enzyme activity. Similarly, Equation (4) predicts that the lower limit of the inhibition curve will not reach zero, that is, complete inhibition, even at infinite cocaine concentration.

Thus, one should select appropriate concentrations of the components to minimize the formation of inhibitor/enzyme or enzyme I/enzyme II conjugates in the absence of the allosteric modulator (i.e., cocaine or bridging nucleic acid) to highlight the effect of the supramolecular structures on the inhibition of the enzyme or the activation of the enzyme cascade. Our model predicts that these conditions are maintained when a concentration of H below K_H is used, thus resulting in a high upper limit for the inhibition-based system or a small lower limit for the enzyme cascade, respectively.

Figure 6 shows the recorded absorbance changes of the ChOx/MB$^+$ system for various concentrations of cocaine at

 © 2010 Wiley-VCH Verlag GmbH & Co. KGaA, Weinheim

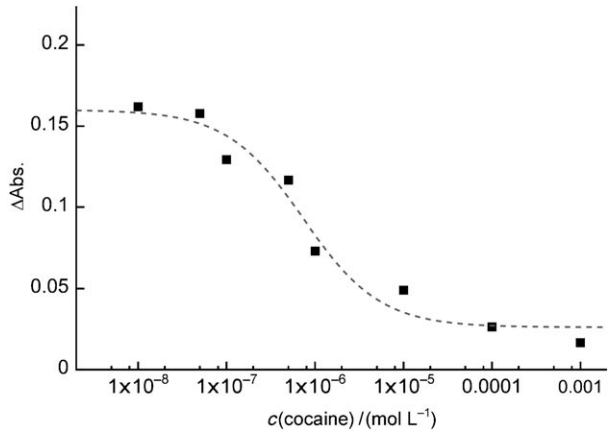

Figure 6. Absorbance changes (ΔAbs at 300 s; squares) as a function of the cocaine concentration and nonlinear fit by using Equation (1) (dashed line). The obtained fitting parameters are given in Table 1.

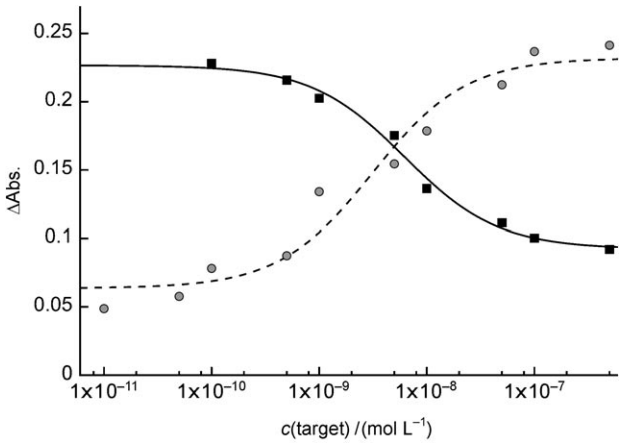

Figure 7. Target DNA binding by the Y-shape probe (ΔAbs at 300 s) and a nonlinear curve fit by the ternary complex assembly model. ChOx/MB^+-modified DNA (black squares, solid line) uses Equation (1) and GOx/HRP-modified DNA (gray circles, dashed line) uses Equation (2).

$t = 300$ s. The nonlinear curve fitting was performed with software "gnuplot" by using Equations (1) and (3). The fitting results and a comparison to the standard logistic fit are shown in Table 1. These results show a significant difference between the two fitting models. The maximum (saturation) value for the logistic fit is considerably smaller than the maximum enzymatic activity derived from the ternary complex model. As mentioned above, this outcome is due to the contribution of the affinity interaction between the two aptamer subunits. This interaction results in an inhibition of the ChOx activity by MB^+, even at a zero concentration for cocaine. The true E_{max} value is only observed in the absence of the MB^+-labeled aptamer subunit (Figure 1). Furthermore, we see a clear difference between the inhibition constant derived from the inflection point of the logistic curve fit x_0 and the target dissociation constant K_T that we yield from the ternary complex fit. The obtained K_D value for cocaine of 4.5 μM and the high cooperativity factor α' support our premise that a simple one-to-one binding model cannot give reasonable results. Instead, a more complex model is necessary to describe the assembly of the aptamer subunits upon cocaine binding.

The ternary complex model was also applied to fit data obtained from the target DNA binding by the Y-shaped structure. In this case, two slightly different equations were employed for the nonlinear regression of the enzyme inhibition and the enzyme cascade [i.e., Eqs. (1) and (2), respectively]. Figure 7 shows the recorded absorbance changes after 300 seconds and the fitted binding curves by using the aforementioned equations. Table 2 gives an overview of the obtained parameters (see the Supporting Information for a complete list including the initial parameter set).

Although, both target DNA sensing systems use quite different reporting mechanisms, that is, the inhibition of ChOx or a cascade of GOx and HRP, the obtained results are strikingly similar. The cooperativity factor α' is almost identical, as is the dissociation constant for the target K_T. Only the dissociation constant K_H for the two probe strands differs slightly. Interestingly, the obtained K_H value is also very similar to the one derived from the assembly of the aptamer subunits. The main difference between the presented systems, therefore, lies in the target compound, which can be a low-affinity ligand such as cocaine or a strongly binding oligonucleotide. In either case, the cooperative assembly of the ternary complex allows sensing of the respective analyte with a sensitivity well below its bimolecular binding constant.

Table 2. Fitted parameters for the target DNA binding by the Y-shaped probe after nonlinear regression with Equations (1) and (2) for the enzyme inhibition or enzyme cascade, respectively.

Parameter	Inhibition	Cascade
K_H [μmol L^{-1}]	0.64	0.16
K_T [μmol L^{-1}]	15.3	18.4
α'	21.1	21. 5
$E_{max,1}$	0.244	–
$E_{max,2}$	–	0.267
reduced χ^2	4.770×10^{-5}	3.199×10^{-4}

Conclusions

The present study has demonstrated that the programmed self-assembly of enzymes by means of DNA nanostructures provides an effective means to control biocatalytic functions that do not occur (under similar experimental conditions) in a random, nonorganized system. The significance of cooperative interactions on the formation of supramolecular structures has been discussed recently.[16] The present study demonstrates the stabilization of supramolecular DNA structures by such cooperative principles. We examined two different nucleic acid-based systems that were designed to form such nanostructures. The first one utilizes the facilitated assembly of two aptamer subunits by cocaine. The second system uses two nucleic acid probe strands to cap-

 © 2010 Wiley-VCH Verlag GmbH & Co. KGaA, Weinheim

ture a third oligonucleotide, that is, the target. The two parts of the biocatalytic arrangement, namely, enzyme and inhibitor or enzyme I and enzyme II, were tethered to the nucleic acids to generate a reporter system. Methylene blue (MB^+) was used to inhibit the catalytic activity of choline oxidase (ChOx); that is, upon the assembly of the nanostructure of aptamer subunits **1** and **2** and cocaine or the probe strands **4** and **5** and target nucleic acid **6**, a decrease in the ChOx turnover would be monitored. In another approach, we used the channeling of H_2O_2 from glucose oxidase (GOx) to horseradish peroxidase (HRP) to report the assembly of the Y-shaped nanostructure, which comprised the probe oligonucleotides **4** and **5**, by the addition of the target DNA **6**. With these systems, we reached a detection limit for cocaine down to 10 nM. The target nucleic acid **6** could be detected at concentrations as low as 0.1 or 0.01 nM for ChOx inhibition or the enzyme cascade, respectively. Furthermore, we have provided a model to describe the assembly process of these programmed nanostructures.

Experimental Section

Chemicals: Bis(sulfosuccinimidyl) suberate (BS^3) was purchased from Pierce Biotechnologies. Monocarboxy methylene blue N-hydroxysuccinimide (NHS) ester was purchased from Emp Biotech. All the other reagents were purchased from Sigma–Aldrich.

Oligonucleotides: The following oligonucleotide sequences were purchased from Sigma–Genosys:

1: 5′ GGGAGTCAAGAACGAA$(CH_2)_6NH_2$ 3′
2: 5′ $NH_2(CH_2)_6$TTCGTTCTTCAATGAAGT GGGACGACA 3′
3: 5′ $NH_2(CH_2)_6$TTCGTTCTTGACTTCCC 3′
4: 5′ GACTACTGCTAAGTT$(CH_2)_6NH_2$ 3′
5: 5′ $NH_2(CH_2)_6$AACTTAGACAGTCATGCTC 3′
5a: 5′ AACTTAGACAGTCATGCTCAAAA 3′
6: 5′ GAGCATGACTGTCAGTAGTC 3′

Optical instrumentation: UV/Vis spectroscopic measurements were carried out on a Shimadzu UV-2401PC spectrophotometer.

Preparation of MB^+-modified strands 1 and 5 and ChOx-linked strands 2–4: An excess of BS^3 linker was added to nucleic acid **2**, **3**, or **4** (1×10^{-4} M) in a phosphate buffer solution (50 μL, 10 mM, pH 7.4). The reaction mixture was shaken for 30 min. The product was purified by separation on microspin (G-25) columns and treated with ChOx (1×10^{-3} M) for 2 h. Nucleic acids **1** and **5** (1×10^{-4} M) in phosphate buffer solutions (10 mM, pH 7.4) were treated separately with MB^+ NHS ester (1×10^{-3} M) for 2 h. The products were purified by ultrafiltration on microspin (G-25) columns.

Enzyme/inhibitor activity assays: ChOx-modified strands **2** or **4** and MB^+-modified strands **1** or **5** (5×10^{-8} M) were mixed with different concentrations of cocaine or **6** for 30 min at room temperature. $ABTS^{2-}$ (2.5×10^{-5} M), HRP (5×10^{-7} M), and choline chloride (25 mM) were added to reach a final volume of 0.2 mL. Time-dependent absorbance changes were recorded at $\lambda=414$ nm. The reaction was performed in a phosphate buffer solution (10 mM, pH 7.4, 100 mM NaCl).

Hydrolysis of cocaine: The inhibited ChOx system, which comprised the cocaine/aptamer subunit supramolecular structure, was treated with approximately 4 units of butyrylcholinesterase from human serum to hydrolyze the cocaine. The ChOx activity was assayed as described above.

Preparation of the GOx/HRP-modified strands 4 and 5: An excess of BS^3 linker was added to nucleic acid **4** or **5** (1×10^{-4} M) in a phosphate buffer solution (50 μL, 10 mM, pH 7.4). The mixture was shaken for 30 min. The products were purified by separation on microspin (G-25) columns and subsequently treated with GOx (**4**) or HRP (**5**) (1×10^{-3} M) for 2 h, respectively. The products were purified by ultrafiltration on microspin (G-25) columns.

Enzyme cascade activity assays: GOx-modified strand **4** and HRP-modified strand **5** (5×10^{-9} M) were mixed with different concentrations of **6** for 30 min at room temperature. $ABTS^{2-}$ (2.5×10^{-5} M) and glucose (25 mM) were added to reach a final volume of 0.2 mL. Time-dependent absorbance changes were recorded at $\lambda=414$ nm. The reaction was performed in a phosphate buffer solution (10 mM, pH 7.4, 100 mM NaCl).

Influence of catalase on the enzyme cascade: The free enzymes GOx (1×10^{-8} M) and HRP (1×10^{-8} M) were mixed for the assay of the free enzymes. GOx-modified strand **4** (1×10^{-8} M) and HRP-modified strand **5** (1×10^{-8} M) were mixed with **6** (1×10^{-7} M) for 30 min at room temperature for the assay of the Y-shaped DNA-modified enzymes. Different concentrations of catalase, $ABTS^{2-}$ (2.5×10^{-5} M), and glucose (25 mM) were added to reach a final volume of 0.2 mL. Time-dependent absorbance changes were recorded at $\lambda=414$ nm. The reaction was performed in a phosphate buffer solution (10 mM, pH 7.4, 100 mM NaCl).

Acknowledgements

This research is supported by the Israel Science Foundation. C.T. acknowledges the Minerva foundation for a postdoctoral fellowship.

[1] a) J. T. Davis, *Angew. Chem.* **2004**, *116*, 684; *Angew. Chem. Int. Ed.* **2004**, *43*, 668; b) J. Chen, N. C. Seeman, *Nature* **1991**, *350*, 631; c) K. A. Afonin, D. J. Cieply, N. B. Leontis, *J. Am. Chem. Soc.* **2008**, *130*, 93; d) E. Winfree, F. Liu, L. A. Wenzler, N. C. Seeman, *Nature* **1998**, *394*, 539.

[2] a) J. Elbaz, M. Moshe, B. Shlyahovsky, I. Willner, *Chem. Eur. J.* **2009**, *15*, 3411; b) D. Li, B. Shlyahovsky, J. Elbaz, I. Willner, *J. Am. Chem. Soc.* **2007**, *129*, 5804; c) Y. Lu, J. Liu, *Curr. Opin. Biotechnol.* **2006**, *17*, 580; d) D. M. Kolpashchikov, *J. Am. Chem. Soc.* **2008**, *130*, 2934.

[3] a) R. Freeman, Y. Li, R. Tel-Vered, E. Sharon, J. Elbaz, I. Willner, *Analyst* **2009**, *134*, 653; b) B. R. Baker, R. Y. Lai, M. S. Wood, E. H. Doctor, A. J. Heeger, K. W. Plaxco, *J. Am. Chem. Soc.* **2006**, *128*, 3138; c) J. Liu, Y. Lu, *J. Am. Chem. Soc.* **2005**, *127*, 12677; d) M. Levy, S. F. Cater, A. D. Ellington, *ChemBioChem* **2005**, *6*, 2163; e) V. Pavlov, B. Shlyahovsky, I. Willner, *J. Am. Chem. Soc.* **2005**, *127*, 6522; f) M. N. Stojanovic, P. D. Prada, D. W. Landry, *J. Am. Chem. Soc.* **2001**, *123*, 4928; g) R. Gill, R. Polsky, I. Willner, *Small* **2006**, *2*, 1037.

[4] a) M. K. Beissenhirtz, I. Willner, *Org. Biomol. Chem.* **2006**, *4*, 3392; b) J.-S. Shin, N. A. Pierce, *J. Am. Chem. Soc.* **2004**, *126*, 10834; c) W. B. Sherman, N. C. Seeman, *Nano Lett.* **2004**, *4*, 1203; d) J. Bath, S. J. Green, A. J. Turberfield, *Angew. Chem.* **2005**, *117*, 4432; *Angew. Chem. Int. Ed.* **2005**, *44*, 4358; e) Y. Tian, Y. He, Y. Chen, P. Yin, C. Mao, *Angew. Chem.* **2005**, *117*, 4429; *Angew. Chem. Int. Ed.* **2005**, *44*, 4355; f) J. Elbaz, R. Tel-Vered, R. Freeman, H. B. Yildiz, I. Willner, *Angew. Chem.* **2009**, *121*, 139; *Angew. Chem. Int. Ed.* **2009**, *48*, 133.

[5] a) Y. Chen, M. Wang, C. Mao, *Angew. Chem.* **2004**, *116*, 3638; *Angew. Chem. Int. Ed.* **2004**, *43*, 3554; b) B. Yurke, A. J. Turberfield, A. P. Mills, Jr., F. C. Simmel, J. L. Neumann, *Nature* **2000**, *406*, 605; c) W. U. Dittmer, F. C. Simmel, *Nano Lett.* **2004**, *4*, 689.

 © 2010 Wiley-VCH Verlag GmbH & Co. KGaA, Weinheim

[6] a) J. Elbaz, M. Moshe, I. Willner, *Angew. Chem.* **2009**, *121*, 3892; *Angew. Chem. Int. Ed.* **2009**, *48*, 3834; b) Y. Benenson, T. Paz-Elizur, R. Adar, E. Keinan, Z. Livneh, E. Shapiro, *Nature* **2001**, *414*, 430; c) M. N. Stojanovic, T. E. Mitchell, D. Stefanovic, *J. Am. Chem. Soc.* **2002**, *124*, 3555; d) M. N. Stojanovic, D. Stefanovic, *Nat. Biotechnol.* **2003**, *21*, 1069; e) G. Seelig, D. Soloveichik, D. Y. Zhang, E. Winfree, *Science* **2006**, *314*, 1585.
[7] a) B. Shlyahovsky, Y. Li, O. Lioubashevski, J. Elbaz, I. Willner, *ACS Nano* **2009**, *3*, 1831; b) S. Beyer, F. C. Simmel, *Nucleic Acids Res.* **2006**, *34*, 1581; c) K. Rinaudo, L. Bleris, R. Maddamsetti, S. Subramanian, R. Weiss, Y. Benenson, *Nat. Biotechnol.* **2007**, *25*, 795; d) M. N. Win, C. D. Smolke, *Science* **2008**, *322*, 456.
[8] a) J. Muller, C. M. Niemeyer, *Biochem. Biophys. Res. Commun.* **2008**, *377*, 62; b) C. M. Niemeyer, J. Koehler, C. Wuerdemann, *ChemBioChem* **2002**, *2002*, 242.
[9] R. Freeman, E. Sharon, R. Tel-Vered, I. Willner, *J. Am. Chem. Soc.* **2009**, *131*, 5028.
[10] S. Nakayama, L. Yan, H. O. Sintim, *J. Am. Chem. Soc.* **2008**, *130*, 12560.
[11] O. Tacal, I. Ozer, *J. Enzyme Inhib. Med. Chem.* **2006**, *21*, 783.
[12] M. N. Stojanovic, P. de Prada, D. W. Landry, *J. Am. Chem. Soc.* **2000**, *122*, 11547.
[13] W. Xie, C. V. Altamirano, C. F. Bartels, R. J. Speirs, J. R. Cashman, O. Lockridge, *Mol. Pharmacol.* **1999**, *53*, 83.
[14] A. Christopoulos, T. Kenakin, *Pharmacol. Rev.* **2002**, *54*, 323.
[15] a) O. A. Ibrahimi, F. Zhang, S. C. L. Hrstka, M. Mohammadi, R. J. Linhardt, *Biochemistry* **2004**, *43*, 4724; b) T. Costa, Y. Ogino, P. J. Munson, H. O. Onaran, D. Rodbard, *Mol. Pharmacol.* **1991**, *41*, 549.
[16] C. A. Hunter, H. L. Anderson, *Angew. Chem.* **2009**, *121*, 7624; *Angew. Chem. Int. Ed.* **2009**, *48*, 7488.

Received: September 16, 2009
Revised: December 17, 2009
Published online: February 11, 2010

 © 2010 Wiley-VCH Verlag GmbH & Co. KGaA, Weinheim